Spectroscopy of rare gas hydrogen halide complexes

Lawrence S. Bernstein and Joda Wormhoudt

Citation: The Journal of Chemical Physics **82**, 4802 (1985); doi: 10.1063/1.448698
View online: http://dx.doi.org/10.1063/1.448698
View Table of Contents: http://scitation.aip.org/content/aip/journal/jcp/82/11?ver=pdfcov
Published by the AIP Publishing

Spectroscopy of rare gas hydrogen halide complexes

Lawrence S. Bernstein
Spectral Sciences, Inc., Burlington, Massachusetts 01803

Joda Wormhoudt
Aerodyne Research, Inc., Billerica, Massachusetts 01821

(Received 27 December 1984; accepted 6 February 1985)

A recently developed band contour model is used to analyze the gas phase spectra of rare gas hydrogen halide complexes in the region of the hydrogen halide fundamental. The sensitivity of model predicted spectra to variation of major spectroscopic parameters is illustrated for ArHCl. Published spectra from several groups for KrHCl, XeHCl, ArHBr, and XeHBr are considered. The unusual appearance of the XeHCl spectrum is attributed to the large shift of the HCl fundamental frequency $-12.5\ \mathrm{cm}^{-1}$ when complexed to Xe. Through spectral analysis the dissociation energies of these complexes were found to be 214 (KrHCl), 220 (XeHCl), 220 (ArHBr), and $300\ \mathrm{cm}^{-1}$ (XeHBr). The uncertainty in these dissociation energies and comparison to other estimates are discussed.

I. INTRODUCTION

Analyzing the infrared spectra of molecular complexes can yield a wealth of information on their structures, dynamics, and intramolecular potentials.[1–15] This even applies to lower spectral resolution spectra where individual vibration–rotation lines are not resolved.[12–15] Recently, we presented an infrared band contour model applicable to atom-linear molecule complexes.[16] This model was applied to the ArHCl infrared spectrum in the region of the HCl fundamental. ArHCl was an important test case since its infrared spectra has been quantitatively measured at several temperatures,[17–19] its ground state spectroscopic constants are accurately known,[20–22] and a reliable potential surface is available.[23,24] Energy levels and spectroscopic constants for the excited states, while approximate, were based on the Hutson and Howard M5 potential.[23,24] The band contour model showed encouraging quantitative agreement with the absolute spectral transmission measurements as well as their temperature dependence.

In this paper, the model is applied to a variety of rare gas hydrogen halide complexes. These include KrHCl and XeHCl for which M5 potentials[23] have been determined, although with considerable uncertainty attached to their dissociation energies, and ArHBr and XeHBr for which ground state spectroscopic constants have been determined, although only estimates of their dissociation energies and potential surfaces are available.[25–29] Through analysis of available infrared spectra for the complexes[17,18,30,31] we have narrowed the ranges of their possible dissociation energies.

II. SPECTRAL MODEL

A complete description of the spectral model has been presented elsewhere.[16] The key features are summarized here. The transitions considered are those involving absorption of one quantum of vibrational energy by the hydrogen halide and a change of one quantum in the overall rotational level of the complex. The selection rules, line positions, and line strengths are those for a parallel band of a linear triatomic molecule with the spectroscopic constants and strength factors appropriately averaged over the large amplitude bending and stretching modes.

A. Energy levels and spectroscopic parameters

The energy levels, line positions, and line strengths are given by

$$G_{\eta jl} = G_\eta - B_\eta l(l+1) - D_\eta l^2(l+1)^2 + H_\eta l^3(l+1)^3 + f_\eta \omega_b (j+1), \quad (1)$$

$$\omega = \omega_\eta + 2B_\eta m - \alpha_\eta m^2 - 4D_\eta m^3 + 6H_\eta m^5, \quad (2)$$

and

$$S = S_0 \langle \cos\theta \rangle^2_{\eta j} |m| \exp(-G_{\eta jl}/kT)/Q, \quad (3)$$

where η, l, j denote complex stretch, complex rotation, and hydrogen halide libration respectively, G_η is stretching energy, B_η, α_η, D_η, and H_η are rotational constants, ω_b is the ground state bending energy, ω_η is the band center for the η'th stretching state, $m = -l, l+1$ in the P, R branches, respectively, S_0 is the hydrogen halide integrated band strength, θ is the librational angular coordinate, and Q is the dimer partition function. The factor f_η accounts for the reduction of the bending frequency for the excited stretching states ($0 \leqslant f_\eta \leqslant 1$). Explicit formulas for the energy levels and spectroscopic parameters can be found in our earlier paper.[16] Since the rare gas hydrogen halide complexes appear to have local potential minima for both linear structures,[23] the most stable being Rg—HX (Rg = rare gas, HX = hydrogen halide) there is a separate set of spectroscopic constants and energy levels for each linear configuration.

B. Spectral calculations

Comparison to observed dimer absorption spectra requires computation of the dimer absorption optical depth which is defined by

$$-\ln(I/I_0) = \rho_{AB}\sigma_{AB} l, \quad (4)$$

where I_0, and I are incident and transmitted light, respectively, ρ_{AB} is the "AB" dimer density, σ_{AB} is the frequency dependent absorption cross section, and l is path length. For

 0021-9606/85/114802-07$02.10

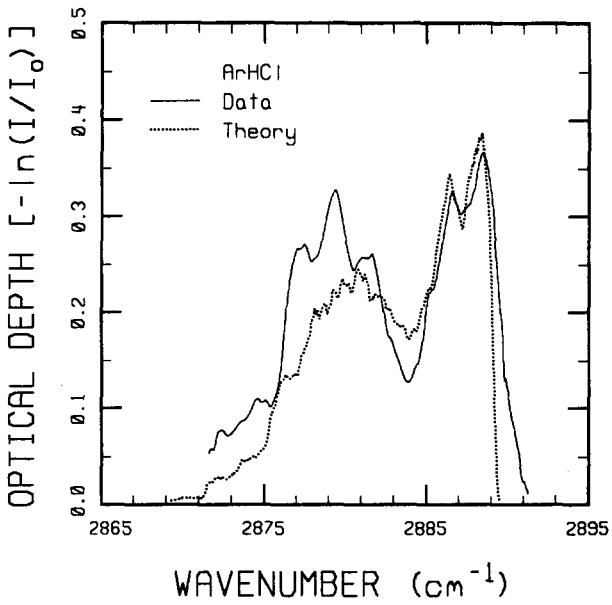

FIG. 1. Comparison of theory to measured (Ref. 18) ArHCl spectrum: 298 K, 250 Torr HCl, 5.01 atm Ar, and 90 cm.

the general case where A = Rg and B = HX the dimer density is related to the dimer equilibrium constant K_{eq} through

$$\rho_{AB} = \rho_A \rho_B K_{eq}, \tag{5}$$

and

$$K_{eq} = \exp\left(\frac{\epsilon}{kT}\right)\left(\frac{h^2}{2\pi\mu kT}\right)^{3/2}\left(\frac{B_{HX}}{kT}\right)Q_{AB}, \tag{6}$$

where ρ_A, and ρ_B are monomer densities, ϵ is dissociation energy, μ is dimer reduced mass, Q_{AB} is the dimer vibration–libration–rotation partition function, and B_{HX} is the hydrogen halide rotational constant. The absorption cross section is related to the line strength and effective spectral resolution $\delta\omega$ (it is assumed that $\delta\omega$ is large compared to line spacing) through

$$\sigma_{AB} = \frac{1}{\delta\omega}\sum_i S_i, \tag{7}$$

where the sum over line strength includes all lines in the frequency interval ω to $\omega + \delta\omega$. We note that it is not necessary to evaluate the dimer partition function in order to predict dimer spectra. This occurs because the dimer optical depth involves the product of line strength [Eq. (3)] and equilibrium constants [Eq. (6)] in which the dependence on Q_{AB} cancels.

C. Model sensitivity to spectroscopic parameters

The effects on spectral predictions due to variation of the spectroscopic parameters are divided into two categories, total integrated intensity and spectral shape. The integrated intensity is most dependent on the dissociation energy, the bending amplitude, and the contribution of the secondary well (i.e., the Rg—XH configuration). The shape is sensitive to the shift of the hydrogen halide fundamental frequency and the vibration rotation constant. The shape also strongly depends on the other rotational constants, however, these are usually well determined from microwave measurements or they can often be adequately estimated.

In order to quantify the effects of varying these spectroscopic parameters we consider the ArHCl spectrum which is shown in Fig. 1. The spectroscopic constants used for this base line spectrum are given in Table I. As discussed in our earlier article, differences between theory and prediction are attributable to uncertainties in removing the underlying continuum spectrum and to model approximations.

The effects of varying intensity factors are displayed in Fig. 2. Increasing the dissociation energy by 40 cm^{-1} increases the integrated intensity by about 30%. Decreasing the ground state bending amplitude by 4° decreases the integrated intensity by around 30%. Removing the secondary well decreases the integrated intensity by approximately 10%.

The effects of varying the shape factors is displayed in Fig. 3. Decreasing the vibration rotation constant by a factor of two noticeably alters the fine structure in the R branch and minimally alters the P branch region. The value for the vibration rotation constant in Table I represents a significant change, about a factor of two increase, from that reported previously[16] and leads to improved agreement with the observed R branch structure. Changing the value for the spectral shift of the HCl fundamental frequency significantly displaces the position of the predicted minimum and noticeably alters the fine structure in both the P and R branches.

TABLE I. Summary of parameter values used in the spectral analysis.

Parameter		ArHCl	KrHCl	XeHCl	ArHBr	XeHBr
Dissociation energy	$\epsilon_1(cm^{-1})$	181.0	214.0	220.0	220.0	300.0
Dissociation energy	$\epsilon_2(cm^{-1})$	146.0	156.0	160.0	200.0	270.0
Bending energy	$\omega_b^{(1)}(cm^{-1})$	32.4	36.2	41.6	25.7	33.2
Spectral shift	$\Delta\omega_0^{(1)}(cm^{-1})$	− 2.0	− 6.5	− 12.5	− 2.0	− 8.0
Spectral shift	$\Delta\omega_0^{(2)}(cm^{-1})$	− 6.5	− 7.5	− 14.5	− 3.0	− 9.0
Bending angle	$\langle\theta_1\rangle_0$(deg)	47.7	40.0	33.9	50.0	34.0
Angular barrier	$V_m(cm^{-1})$	76.0	97.0	128.0	61.0	100.0
Rotation constant	$B_0^{(1)}(10^{-2}\,cm^{-1})$	5.76	4.00	3.31	3.69	1.73
Vibration–rotation	$\alpha_0^{(1)}(10^{-4}\,cm^{-1})$	4.0	0.80	0.66	0.37	0.52
Centrifugal distortion	$D_0^{(1)}(10^{-7}\,cm^{-1})$	6.08	2.46	1.27	4.15	0.282
Higher order rotation	$H_0^{(1)}(10^{-12}\,cm^{-1})^a$	24.3	5.45	2.87	4.00	0.202
Band strength	$S_0(cm^{-1}atm^{-1}$ at STP)	155.0	155.0	155.0	39.3	39.3

[a] Estimated from Table I of Ref. 16.

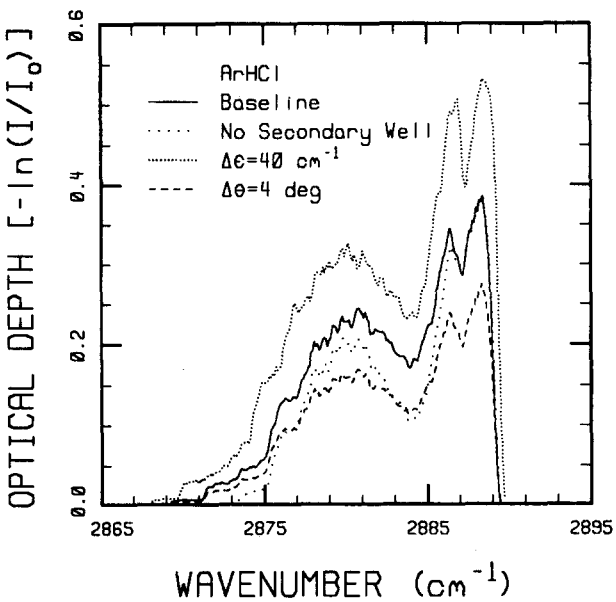

FIG. 2. Sensitivity of predicted ArHCl spectrum to variations in the integrated intensity parameters.

The sensitivity of the predicted spectrum to changes in the spectroscopic parameters indicates the potential usefulness of lower spectral resolution measurements of dimer infrared spectra for extracting information about intermolecular potentials. It also points out the accuracy requirements for the measurements. Using ArHCl as an example, a 10% uncertainty in determining the absolute optical depths would result in a 13 cm^{-1} uncertainty in the dissociation energy (this assumes all other parameters are precisely known). From Fig. 3, we find that it is difficult to distinguish changes in the dissociation energy from changes in the bending angle amplitude at a single temperature. However, if spectral measurements can be performed at two substantially different temperatures, both quantities can be simultaneously determined. For ArHCl the contribution of the secondary well is small and would, therefore, require quite accurate optical depth measurements in order to extract reliable information. The accuracy of the shape function depends primarily on measurement spectral resolution.

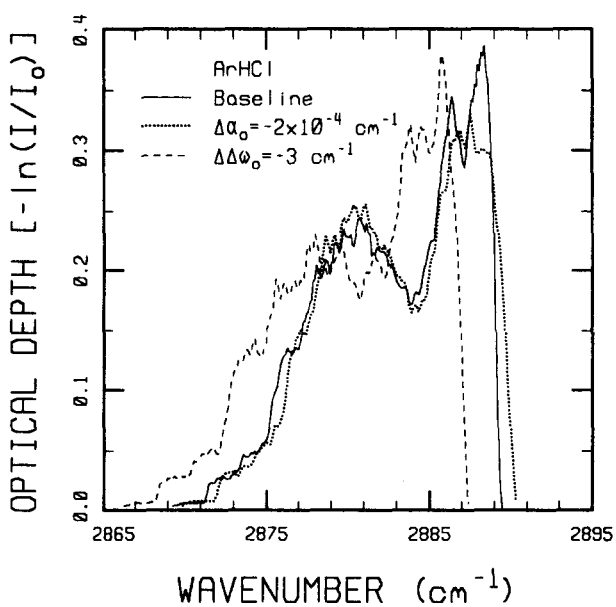

FIG. 3. Sensitivity of predicted ArHCl spectrum to variations in the spectral shape parameters.

D. Estimation of spectroscopic parameters for the secondary well

In the previous paper we did not present explicit formulas for estimating the ground state spectroscopic parameters of the secondary well. We scale the spectroscopic parameters for the secondary well directly from those of the primary well through the following relations,

$$R_e^{(2)} = R_e^{(1)} - \Delta R_e, \tag{8}$$

$$B_0^{(2)} = B_0^{(1)}[R_e^{(1)}/R_e^{(2)}]^2, \tag{9}$$

$$\alpha_0^{(2)} = \alpha_0^{(1)}[R_e^{(1)}/R_e^{(2)}], \tag{10}$$

$$D_0^{(2)} = D_0^{(1)}(\epsilon_1/\epsilon_2)[B_0^{(2)}/B_0^{(1)}]^2, \tag{11}$$

$$\langle\theta_2\rangle = \langle\theta_1\rangle\{V_m/[V_m - (\epsilon_1 - \epsilon_2)]\}^{1/4}, \tag{12}$$

$$\omega_b^{(1)} = a_0(V_m B_{HX})^{1/2}, \tag{13}$$

$$\omega_b^{(2)} = \omega_b^{(2)}\{[V_m - (\epsilon_1 - \epsilon_2)]/V_m\}^{1/2}, \tag{14}$$

where the subscripts or superscripts "1" and "2" denote the primary and secondary well, respectively, R_e is equilibrium bond length, ΔR_e is change in bond length, V_m is the maximum height of the angular barrier, and a_0 is a constant which was determined from analysis of the ArHCl spectrum ($a_0 = 1.14$). While these relations are quite approximate and based on simple harmonic oscillator behavior, given the relatively small contribution of the secondary well to the infrared spectra a more accurate approach is not warranted. The value of ΔR_e was taken as $\Delta R_e = 0.05$ Å for all Rg–HX cases and was estimated from the *ab initio* potential of Vliegenthart and Rozendaal for ArHCl.[23]

III. SPECTRAL COMPARISONS

The spectroscopic parameters in Table I were taken from previous measurements or estimates where possible, and those remaining, most importantly the dissociation energies, were determined by best fit to the infrared spectra. In all cases the ground rotational constants B_0 and D_0 and the bending amplitude $\langle\theta\rangle_0$ are well known from microwave measurements.[23,25–29] The integrated band strengths S_0 for HCl and HBr are also known.[32] For KrHCl and XeHCl initial guesses for the dissociation energies, ϵ_1 and ϵ_2, the angular barrier V_m and the bending energy ω_b were based on their M5 potentials. Due to the stated uncertainty in these potentials, particularly in regard to the dissociation energy, these parameters were varied to improve the agreement with the observed infrared spectra. For ArHBr there was much less information on the surfaces to guide our initial estimates for ϵ_1, ϵ_2, V_m, and ω_b. These parameters were adjusted until satisfactory agreement with the observed spectrum was achieved. In all cases the spectral shift of the hydrogen halide fundamental frequency for the primary well $\Delta\omega_0^{(1)}$ was fixed at or near the minimum in the observed spectrum, and the secondary shift, $\Delta\omega_0^{(2)}$ was allowed to vary from $\Delta\omega_0^{(1)}$ to achieve an improved spectral shape. Due to the relatively

small contribution of the secondary well we emphasize that the values for all the parameters of that well are highly uncertain.

The infrared data used in the analysis originates from two groups. Miziolek and Pimentel[30,31] measured the ArHBr spectrum at various temperatures from 212 K to room temperature and at a spectral resolution of about 2 cm^{-1}. Rank and co-workers[17,18] measured room temperature spectra for all the complexes at a high spectral resolution, which due to the pressures used in the absorption cell resulted in a pressure broadened effective resolution of order 0.1 cm^{-1}. Rank and co-workers also measured the XeHCl spectrum at 195 K.

A. XeHCl and KrHCl

A comparison of the calculated and observed room temperature XeHCl spectrum is shown in Fig. 4. Comparably good agreement was obtained in comparison to the 195 K spectrum (not shown here). The dissociation energy determined from these comparisons is 220 cm^{-1} which can be compared to that for the M5 surface of 264 cm^{-1}. While there is certainly some uncertainty associated with the value obtained from the infrared spectral analysis, we estimate it to be less than 44 cm^{-1} and probably closer to ± 20 cm^{-1}. A value as high as 264 cm^{-1} would result in about a 35% increase in the predicted integrated intensity.

It is interesting to compare the XeHCl and ArHCl spectra. They are quite dissimilar. ArHCl has well defined P and R branch maxima, characteristic of linear molecule parallel bands, and XeHCl does not. The reasons for this can be visualized by considering some of the component subbands of the XeHCl spectrum shown in Fig. 5. There are separate sequences of bands for each linear configuration as well as for each isotope, $XeH^{35}Cl$ and $XeH^{37}Cl$. Only a few components of the primary sequences for the most stable linear structure and the most abundant isotope are shown. Within

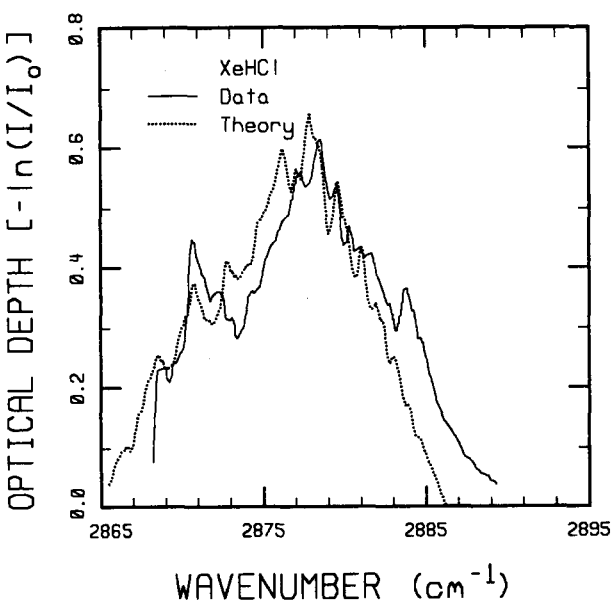

FIG. 4. Comparison of theory to measured (Ref. 18) XeHCl spectrum: 298 K, 250 Torr HCl, 2.05 atm Xe, and 90 cm.

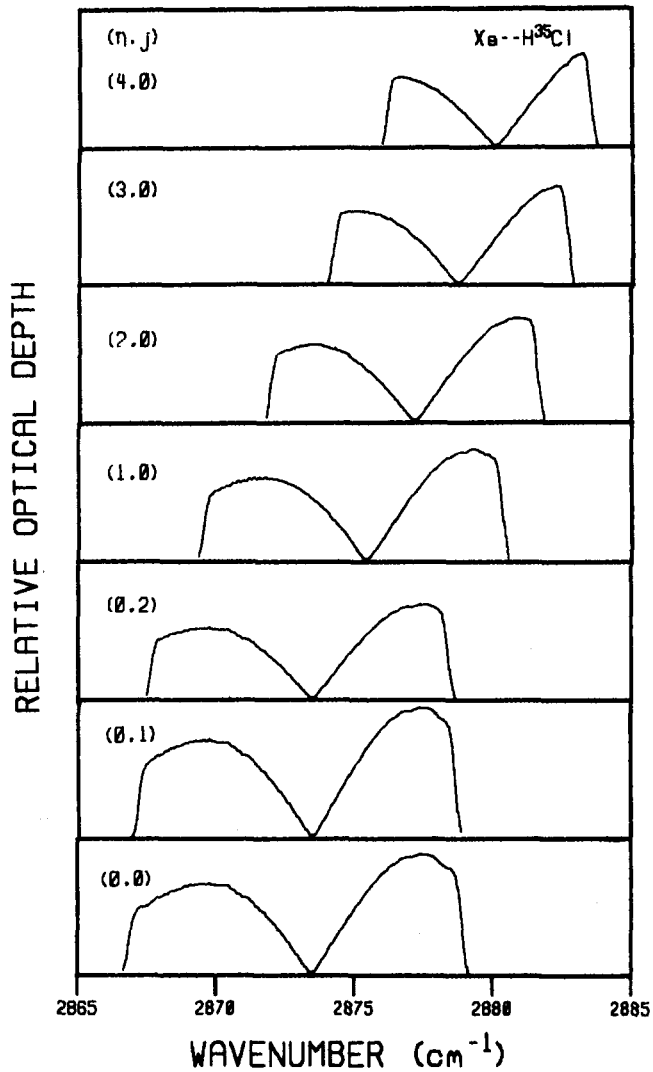

FIG. 5. Representative contributions to the XeHCl spectrum.

a sequence the width of each band decreases with increasing stretch η or libration j quantum numbers, and there are sharp P and R branch cutoffs. This behavior is due to the finite number of rotational states which exist below the centrifugal barrier to dissociation. As the stretch or libration quantum are increased, there are fewer rotational states left below the centrifugal barrier, hence a decrease in the subband width. We attribute the spikey features observed in the XeHCl spectrum to the sharp P, R branch cutoffs.

The spectral shift of the HCl fundamental frequency is much larger for XeHCl ($\Delta\omega_0^{(1)} = -12.5$ cm^{-1}) than for ArHCl ($\Delta\omega_0^{(1)} = -2.$ cm^{-1}). The effect of the large shift on the predicted spectrum is shown by the "η" sequence in Fig. 5. As the stretching quantum level increases, the average separation of the rare gas and hydrogen halide also increases. This leads to a decreased interaction potential between the rare gas and hydrogen halide and therefore to a decrease in the spectral shift. The explicit dependence of the spectral shift on the stretching quantum state was derived previously. Because the ground state spectral shift for XeHCl is so large, each succeeding band origin in the η sequence is significantly displaced from the previous one. This effectively uncorrelates the P and R branch maxima between subbands and

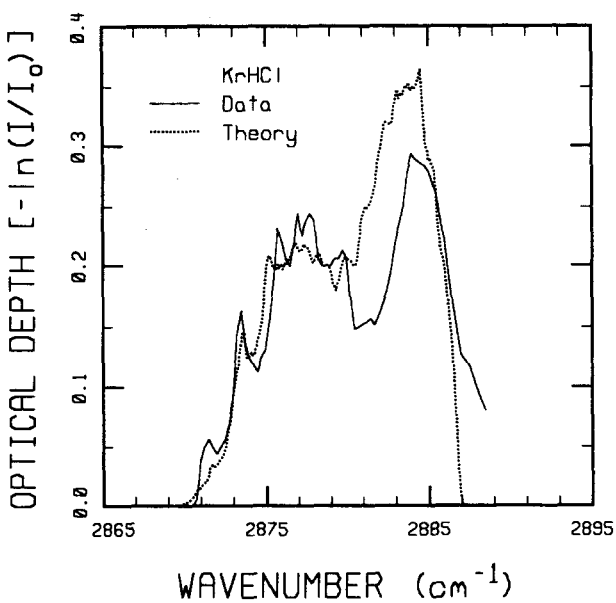

FIG. 6. Comparison of theory to measured (Ref. 18) KrHCl spectrum: 298 K, 250 Torr HCl, 1.84 atm Kr, and 90 cm.

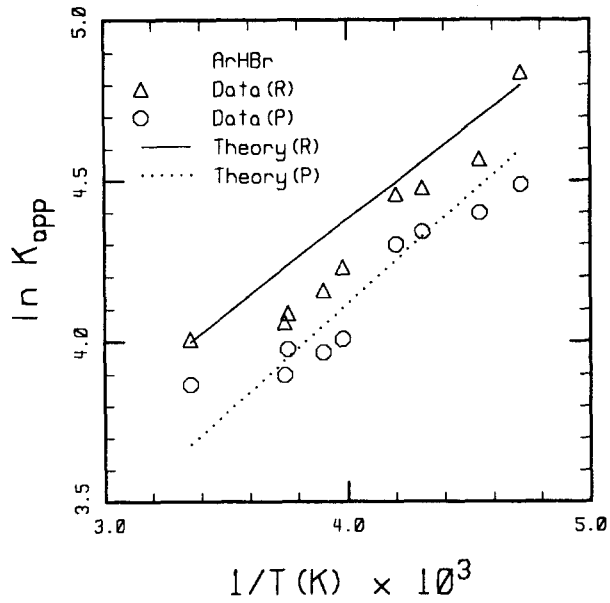

FIG. 7. Comparison of theory to measured (Refs. 30 and 31) temperature dependence of the apparent equilibrium constant for ArHBr.

results in the unusual appearance of the XeHCl spectrum. For ArHCl the shift is sufficiently small that the P and R branch maxima for the subbands significantly overlap and thus the appearance of a typical parallel band is maintained.

A comparison of the calculated and observed room temperature KrHCl spectrum is displayed in Fig. 6. The general appearance of this spectrum is intermediate between those for ArHCl and XeHCl. This is expected since the spectral shift for KrHCl is about midway between that for the other two. The dissociation energy for the M5 potential of 214 cm^{-1} was found to be consistent with the observed spectra.

B. ArHBr and XeHBr

Miziolek and Pimentel[31] measured the temperature dependence of the P and R branch peak absorption for ArHBr from 212 K to room temperature. They expressed the absorption in terms of an apparent equilibrium constant, K_{app}, which was defined as the measured optical depth divided by the product of path length and monomer concentrations. Using an ArHBr dissociation energy of 220 cm^{-1} we compare the calculated and measured temperature dependence of the apparent equilbrium constant in Fig. 7. We can compare this value of the ArHBr dissociation energy to that estimated by Keenan and co-workers.[27] Their estimate of 206 cm^{-1} is close to the value of 220 cm^{-1} which best fit the infrared data. They used a procedure, originally applied by Novick and co-workers,[33] which uses isotopically substituted molecular beam rotational spectra to correct for a significant bend stretch interaction energy. This procedure yields dissociation energies which agree reasonably well with those determined through Hutson and Howard's surface fitting method for other complexes.

A comparison to Miziolek and Pimentel's[30] room temperature ArHBr spectrum is shown in Fig. 8. In this comparison the predicted P, R branch peaks are about 20% higher than the observed peaks. However, in comparing to the room temperature data in Fig. 7 for the apparent equilibrium constant and using the same spectroscopic constants as in the spectral comparison, we predicted about 20% lower than the observed P branch peak. This discrepancy is likely related to the difficulties in removing the underlying spectral base line. For the apparent equilibrium constant data the base line contribution was removed (i.e., estimated) by Miziolek and Pimentel, where as we estimated the base line for the spectral comparison. A comparison to the higher spectral resolution room temperature ArHBr spectrum of Rank and co-workers is shown in Fig. 9. A spectral resolution of 0.3 cm^{-1} was used for the calculated spectrum although it

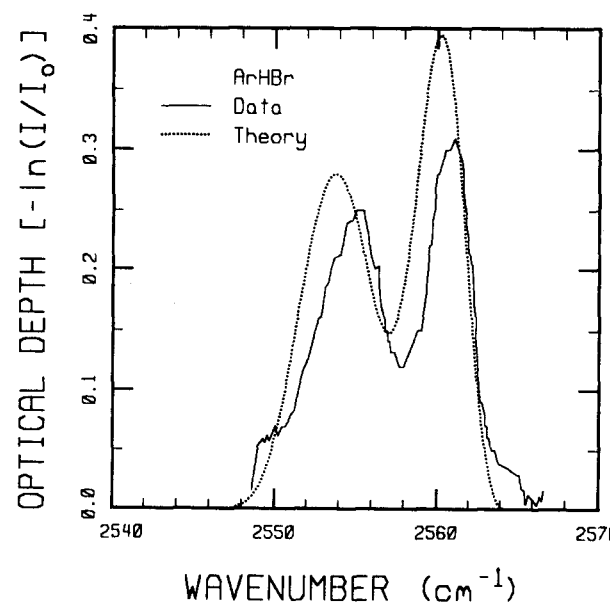

FIG. 8. Comparison of theory to measured (Ref. 30) ArHBr spectrum: 298 K, 6.95 Torr HBr, 0.998 atm Ar, and 460 m.

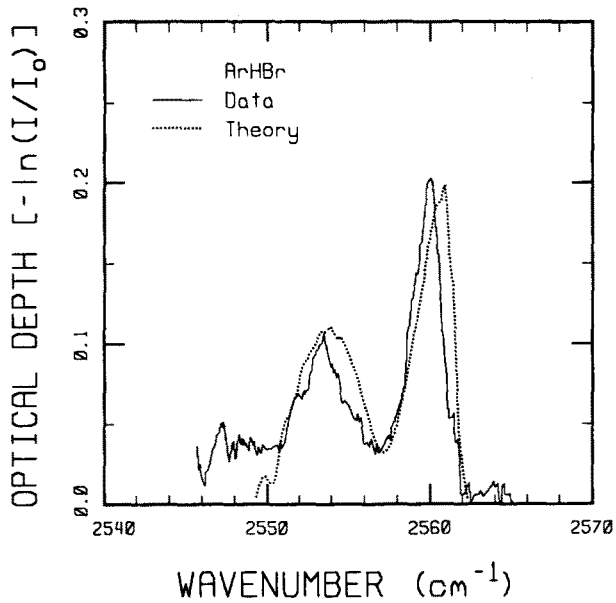

FIG. 9. Comparison of theory to measured (Ref. 18) ArHBr spectrum: 298 K, 250 Torr HBr, 5.02 atm Ar, and 90 cm.

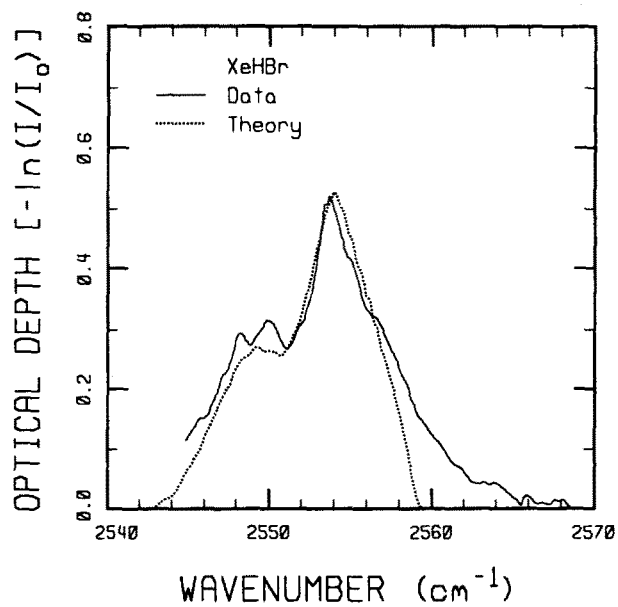

FIG. 10. Comparison of theory to measured (Ref. 18) spectrum: 298 K, 250 Torr HBr, 2.18 atm Xe, and 90 cm.

appears that the data show fine structure at a somewhat higher spectral resolution. From the well defined minimum in the ArHBr spectrum the spectral shift of the HBr fundamental is found to be $\Delta\omega_0^{(1)} = -2$ cm^{-1}. This is the same small shift as was found for the HCl fundamental in ArHCl and is the reason for the distinct P, R branch maxima in ArHBr.

The degree of asymmetry in the predicted ArHBr spectra is a sensitive function of the vibration rotation constant α_0. For $\alpha_0 = 0$ the P and R branches are approximately equal in width and peak height. As α_0 is increased the P branch widens and decreases in peak height and the R branch narrows and increases in peak height.

Using a XeHBr dissociation energy of 300 cm^{-1} we compare the calculated and observed room temperature spectra in Fig. 10. Kukolich and Campbell[28] have estimated the dissociation energy at 244 cm^{-1}. However, their estimate does not include the effect of the bend stretch interaction which, when included, increases the dissociation energy. Estimating this effect leads to a dissociation energy of 320 cm^{-1}, not significantly different from the value of 300 cm^{-1} determined here from the infrared spectrum.

IV. CONCLUDING REMARKS

We have shown that a relatively simple spectral model yields good quantitative agreement with observed spectra for a wide variety of rare gas hydrogen halide complexes. As outlined here and in our previous paper the model can be applied to the general case of an atom-linear molecule complex with local potential minima corresponding to linear structures. Currently we are generalizing the model to apply to linear molecule—linear molecule complexes with linear potential minima. In particular, we are interested in the N_2HCl complex for which the ground state rotational constants are well determined[34] and the room temperature infrared spectrum has been measured at 2 cm^{-1} spectral resolution.[30] Based on a very preliminary analysis of that spectrum we estimate a dissociation energy for N_2HCl of about 270 cm^{-1}.

ACKNOWLEDGMENTS

The authors thank the Atmospheric Sciences Division of the National Science Foundation, Spectral Sciences Incorporated and Aerodyne Research Incorporated for sponsoring this work.

[1]R. J. LeRoy and J. van Kranendonk, J. Chem. Phys. **61**, 4750 (1974).
[2]H. Kreek and R. J. LeRoy, J. Chem. Phys. **63**, 338 (1975).
[3]J. K. Cashion, J. Chem. Phys. **45**, 1656 (1966).
[4]R. G. Gordon and J. K. Cashion, J. Chem. Phys. **44**, 1190 (1966).
[5]A. Watanabe and H. L. Welsh, Phys. Rev. Lett. **13**, 810 (1964).
[6]A. Kudian, H. L. Welsh, and A. Watanabe, J. Chem. Phys. **43**, 3397 (1965).
[7]A. Kudian, H. L. Welsh, and A. Watanabe, J. Chem. Phys. **47**, 1553 (1967).
[8]A. Kudian and H. L. Welsh, Can. J. Phys. **49**, 230 (1971).
[9]A. R. W. McKellar and H. L. Welsh, J. Chem. Phys. **55**, 595 (1971).
[10]A. R. W. McKellar and H. L. Welsh, Can. J. Phys. **50**, 1458 (1972).
[11]A. R. W. McKellar and H. L. Welsh, Can. J. Phys. **52**, 1082 (1974).
[12]G. Henderson and G. E. Ewing, Mol. Phys. **27**, 903 (1974).
[13]G. Henderson and G. E. Ewing, J. Chem. Phys. **59**, 2280 (1973).
[14]R. D. Pendley and G. Ewing, J. Chem. Phys. **78**, 3531 (1983).
[15]C. A. Long and G. E. Ewing, J. Chem. Phys. **58**, 4824 (1973).
[16]L. S. Bernstein and J. Wormhoudt, J. Chem. Phys. **80**, 4630 (1984).
[17]D. H. Rank, P. Sitaram, W. A. Glickman, and T. A. Wiggins, J. Chem. Phys. **39**, 2673 (1963).
[18]D. H. Rank, B. S. Rao, and T. A. Wiggins, J. Chem. Phys. **37**, 2511 (1962).
[19]A. W. Miziolek and G. C. Pimentel, J. Chem. Phys. **65**, 4462 (1976).
[20]S. E. Novick, P. Davis, S. J. Harris, and W. Klemperer, J. Chem. Phys. **59**, 2273 (1973).
[21]S. E. Novick, K. C. Janda, S. L. Holmgren, M. Waldman, and W. Klemperer, J. Chem. Phys. **65**, 1114 (1976).
[22]J. M. Hutson and B. J. Howard, J. Chem. Phys. **74**, 6520 (1981).
[23]J. M. Hutson and B. J. Howard, Mol. Phys. **45**, 769 (1982).
[24]J. M. Hutson and B. J. Howard, Mol. Phys. **43**, 493 (1981).
[25]K. C. Jackson, P. R. Langridge-Smith, and B. J. Howard, Mol. Phys. **39**, 817 (1980).
[26]W. G. Read and E. J. Campbell, J. Chem. Phys. **79**, 1669 (1983).

[27]M. R. Keenan, E. J. Campbell, T. J. Balle, L. W. Buxton, T. K. Minton, P. D. Soper, and W. H. Flygare, J. Chem. Phys. **72**, 3070 (1980).
[28]S. G. Kukolich and E. J. Campbell, Chem. Phys. Lett. **94**, 73 (1983).
[29]M. R. Keenan, L. W. Buxton, E. J. Campbell, T. J. Balle, and W. H. Flygare, J. Chem. Phys. **73**, 3523 (1980).
[30]A. W. Miziolek, Ph.D. dissertation, University of California, Berkeley, 1976.
[31]A. W. Miziolek and G. C. Pimentel, J. Chem. Phys. **66**, 3840 (1977).
[32]L. S. Rothman, A. Goldman, J. R. Gillis, R. R. Gamache, H. M. Pickett, R. L. Poynter, N. Husson, and A. Chedin, Appl. Opt. **22**, 1616 (1983).
[33]S. E. Novick, S. J. Harris, K. C. Janda, and W. Klemperer, Can. J. Phys. **53**, 2007 (1975).
[34]R. S. Altman, M. D. Marshall, and W. Klemperer, J. Chem. Phys. **79**, 57 (1983).